

Evaluation of the sterilization effect of a new mercury-free UVC light source

Han Gao^{a,b}, Tongkuo Yuan^{b,c}, Jian Zhao^d, Hongye Liu^e, Huancai Yin^{a,b,*}

^a University of Science and Technology of China, Hefei, Anhui 230026 China

^b CAS Key Lab of Bio-Medical Diagnostics, Suzhou Institute of Biomedical Engineering and Technology, Chinese Academy of Sciences, Suzhou, Jiangsu 215163 China

^c School of Life Sciences, Shanghai University, Shanghai 200433 China

^d NovelUv Co., Ltd, Shanghai 201108 China

^e Clinical Laboratory, Changchun Center Hospital, Jilin, Changchun 130051 China

*Corresponding author, e-mail: yinhc@sibet.ac.cn

Received 13 May 2019

Accepted 29 Oct 2019

ABSTRACT: So far, short-wave UV produced by low-pressure mercury lamps has been widely applied in sterilization, wastewater treatment, and bioassays, which could be due to its low cost, high conversion efficiency, and small size. However, metal pollution is caused by the inevitable releasing of mercury. In this study, a new mercury-free lamp was developed, which generated UV light by the electron beam excitation (EBE) of $\text{YPO}_4:\text{Bi}^{3+}$ under vacuum conditions. Such lamps emit light at 241 nm and possessed a photoelectric effect. Excellent sterilization effect was obtained in *Candida albicans*, *Staphylococcus aureus*, *Pseudomonas aeruginosa*, and *Escherichia coli*, in the absence of ozone. These effects positively correlated with the treatment distances and time. Furthermore, oxidative stress was found to play a major role in the sterilization process of our light sources, since no production of ozone was detected during each treatment. After all, EBE lamps could be a promising tool for sterilization, and our results provided the theoretical basis for its microorganism-killing effects.

KEYWORDS: UV, mercury-free lamp, electron beam excitation (EBE) UV lamp, ozone-free, oxidative stress

INTRODUCTION

Nowadays, UV light sources have been widely applied in industrial, agriculture, and medical fields, due to their fluorescent, biological, photochemical and photoelectric effects¹. In particular, short-wave UV with wavelengths of 200–280 nm has been found useful in sterilization, wastewater treatment and biological detection². Among them, low-pressure mercury lamps producing 254 nm UV light were mostly accepted, which could be due to their long lifetime, high photoelectric conversion efficiency, mature manufacturing process, and low cost³. Unfortunately, these lamps are being criticized for their releasing of mercury, which cause irreversible fatal damage to living organisms⁴. According to Minamata Treaty, mercury-containing UV light sources will be gradually replaced in 2020. Thus more and more attentions are being paid on the development of mercury-free lamps.

The first developed light sources are mainly light-emitting diodes (LEDs), which have advantages of long life, small size, short start-up time,

and no pollution^{5,6}. Despite the long-term development, UVC-producing LEDs are limited by their complicated manufacturing process, high cost, low photoelectric conversion efficiency, and severe heat radiation⁷. In fact, the thermal emission cathode produced by LG Company, which are of the most matured manufactory techniques, only exhibits a low photoelectric conversion efficiency at 2%. Hence an efficient, non-polluting, and long-lifetime UV sources are still in demand.

Based on the recent publications, UV light could be generated by electron beam excitation of phosphate, rare earth-doping material and ZnO ⁸. With similar mechanisms, Oto et al developed new UV lamps by electron beam excitation of AlGaIn quantum wells, which exhibited a high power of 100 mW at 240 nm⁹. Max Shatalov et al used AlGaIn to develop a UV light source with a wavelength of 278 nm¹⁰. Compared with UV LED, EBE-UV light sources possessed simple production processes, no thermal effect, and high photoelectric conversion efficiency, thus exhibiting a promising application

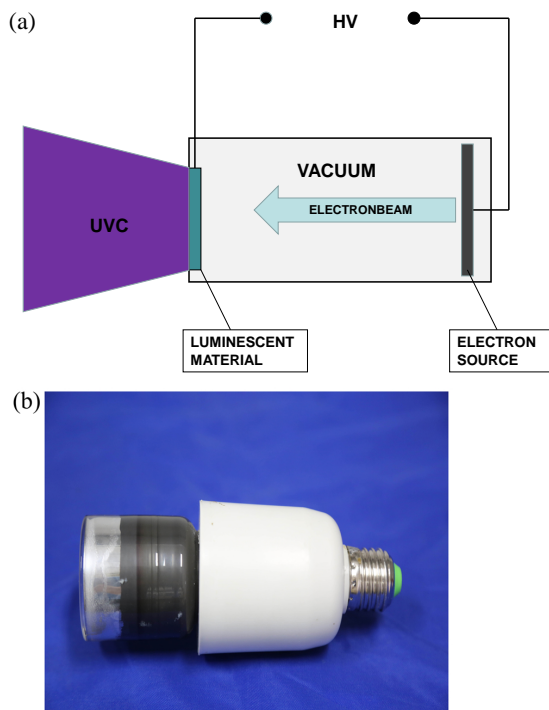


Fig. 1 (a) Schematic diagram of $\text{YPO}_4:\text{Bi}^{3+}$ EBE-UV lamp, HV = high voltage; (b) UV lamp body diagram.

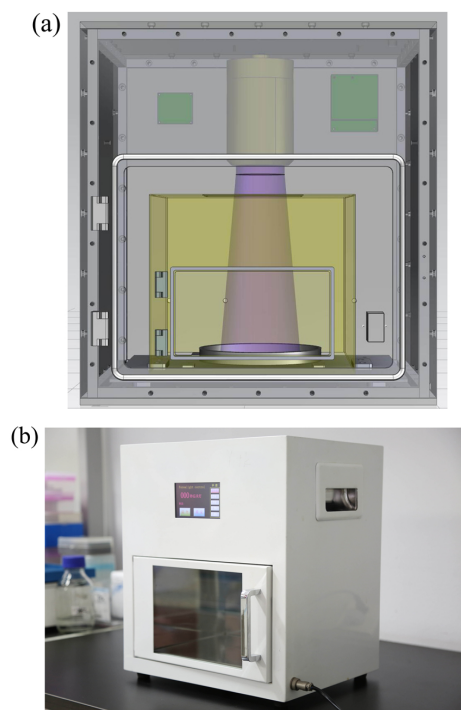


Fig. 2 (a) Schematic diagram of sterilization device; (b) physical map of the equipment.

prospect^{11,12}.

In this study, a small sterilization device was produced with an EBE-UV light source. After characterization of photoelectric conversion efficiency and wavelength, the sterilization properties of this lamp were tested with four microorganisms, including *Candida albicans*, *Staphylococcus aureus*, *Pseudomonas aeruginosa*, and *Escherichia coli*. After then, the main sterilization mechanism of this lamp was detected, to provide the basis for its application in sterilization.

MATERIALS AND METHODS

EBE-UV characterization

The EBE-UV light was produced by electron beam excitation on $\text{YPO}_4:\text{Bi}^{3+}$, and the cold cathode is protected by vacuum environment⁴. In brief, the electrons hit the matrix of $\text{YO}_4:\text{Bi}^{3+}$, causes energy transfer, and excites the fluorescence. With specific optical filter, the wavelength of UV would be limited around 241 nm. By DC Ammeter and Voltmeter, the input power of the UV lamp is 1.3 W, and output power is determined to be 52.13 mW. The photoelectric conversion rate η is calculated according to $\eta = (P_{\text{light}}/P_e) \times 100\%$, where P_{light} and P_e are

the electrical and optical powers, respectively. After calculation, η should be 4.01%.

The schematic and digital illustrations of the lamp are shown in Fig. 1. Its emission spectra were evaluated by a UV spectrometer (Gentec, Florida, USA) in a wavelength range of 200–360 nm. Irradiance power of EBE-UV was measured using a PH100-SiUV Probe accumulated UV meter (Ushio Inc., Japan), after the switch was turned on, the UV meter was set as zero first. Then the irradiance power was randomly detected at 5 different positions of the same height to calculate the average value.

Sterilization device

To test the efficiency of UV light source, a small sterilizer with adjustable distance and treatment time was designed. The structure is shown in Fig. 2.

The sterilizer consists of two parts: tank and shell. The tank was made of corrosion-resistant stainless-steel material (ISO11), with a hole in the upper field. The light sources located inside the shell, right on the upper of the tank holes. The lighting time, interval time, and automatic light-off could be controlled automatically. A transparent viewing window is present on the outer shell, to observe

the entire illumination process. Tin foil was used to cover the shading treatment on the observation window, to avoid the light resurrection during UV treatment. Finally, adjust the distances between the light sources and the plane of the lowest-end plates, to determine the sterilization characteristics.

Culture of microorganisms

C. albicans (ATCC10231), *S. aureus* (ATCC25923), *P. aeruginosa* (ATCC9027), and *E. coli* (ATCC25922) obtained from American Type Culture Collection, were cultured at 37 °C in tryptic soy broth (pH 7.2, BD Diagnosis Systems, Sparks, MD)¹³⁻¹⁵. All the bacteria and yeast kept on a rotary shaker at 220 rpm were cultivated for 8 h. The concentration of cells was 10⁹ CFU/ml as assessed by 600 nm absorption.

Evaluation of sterilization effect

Microorganisms, including yeast (*C. albicans*), Gram-positive bacteria (*S. aureus*), and Gram-negative bacteria (*E. coli* and *P. aeruginosa*), were used to evaluate the sterilization effect of EBE-UV. After reaching the set concentrations of 10⁹ CFU/ml, the four strains of microorganisms were diluted by 1:10 000¹⁶. 100 µl of dilution was cultured on the solid nutrient agar medium, and then immediately placed in the sterilization device. All agar media were treated with UV at 15 cm from the UV light source at 37 °C. According to the tolerance of each strain, different time gradients were used for *C. albicans* (0.0, 1.0, 2.0, 3.0, and 4.0 min), *P. aeruginosa* (0.0, 1.0, 1.5, 2.0, and 2.5 min), *S. aureus* (0.0, 0.5, 1.0, 1.5, 2.0, 2.5, 3.0, and 3.5 min), and *E. coli* (0.0, 5.0, 10.0, 15.0, 20.0, 25.0, 30.0, 35.0, and 40.0 s). Then the survived colonies were counted and compared with untreated control. The differences were divided by the total colonies, and the results were defined as the disappearance rate. The obtained values were plotted against the irradiation dose (K , (mWs/cm²)) of UV, which was calculated as $K = I \times T/10^3$, where I and T are the irradiation intensity (µW/cm²) and irradiation time (s), respectively. To prevent cells from reactivation, the processes of UV treatment and cultivating were shaded away from light.

Intracellular ROS assay

After sterilization, the microorganisms on the plate were scraped off with 1.0 ml PBS. About 100 µl of the treated suspensions were taken out for total number counting, and the remaining suspensions were collected into 1.5 ml eppendorf

tubes (EP), to measure intracellular ROS with commercial Kits (Beyotime, China)¹⁷. 10 µm 2,7-dichlorodihydrofluorescein diacetate (DCFH-DA) was added to the treated suspensions and incubated for 20 min at 37 °C. Then the cells were washed and suspended in 1.0 ml of PBS. The pictures of accumulated 2',7'-dichlorofluorescein (DCF) inside cells were taken with a digital camera (Olympus Corporation, Tokyo) and a Zeiss axiophot fluorescence microscopy (Carl Zeiss, Oberkochen, Germany) with a green filter. After then, the fluorescence of suspension was detected with a Multi-Mode microplate Reader (BioTek, US) using an excitation/emission wavelength of 488/525 nm. Relative fluorescence intensity (RFI) of the intracellular ROS level was normalized to the total number of microorganism¹⁸, and then expressed as the fold increase of control group.

$$RFI = \frac{DCF_{EX}/(1 - \text{Disappearance \%})}{DCF_{Control}}$$

where DCF_{EX} and DCF_{Control} are the detected fluorescence of the treated groups and the control group, respectively.

Ozone content detection

The light resource of the UV sterilizer was fixed at 15 cm from the bottom of the plate. Since all the microorganisms died after 20 min irradiation. The ozone production was detected after then. Ozone instrument (JSA8-O3, Shenzhen, China) was used to detect the ozone content at 6 random points to obtain an average value. The enclosed space of this device is 15 cm in height, 23 cm in length, 10 cm in width. The total volume is about 3.45 l. As a positive control, the ozone produced by an ordinary 254 nm lamp (TUV, 8 W, Philips) was detected in the same condition, and the results indicated a 2.7 ppm production of ozone.

DNA damage analysis

After UVC irradiation for indicated time, the four microorganisms were collected and extracted for their DNA with a commercial kit. The degree of DNA damage was determined by the alkaline version of the Comet Assay (single-cell gel electrophoresis SCGE) as described by Lanier et al¹⁹. The irradiation time was selected for each microorganism with the occurrence of significant death. The obtained comets were visualized with a fluorescent microscope (Carl Zeiss, Oberkochen, Germany) at 40 × magnification (Achromplan and ECPlan-Neofluar objectives) with the red filter (excitation 546 nm and

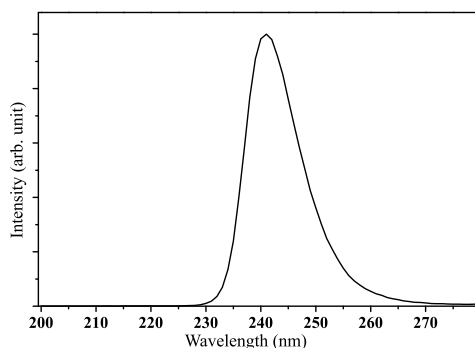


Fig. 3 Emission spectra of $\text{YPO}_4:\text{Bi}^{3+}$ EBE-UV lamp.

Table 1 Radiation intensity at different distance (DIST) from the lighting tube.

DIST/cm	3	6	9	12	15
Irradiance ($\mu\text{W}/\text{cm}^2$)	651.1	280.6	139.1	84.2	55.5

emission 590 nm). The obtained images were analysed using AxioVision software version 4.7.2 (Carl Zeiss, Oberkochen, Germany).

Statistical analysis

All data represent here are mean \pm SD of three independent experiments with each in triplicate ($n = 9$). Statistical analysis was performed using SPSS Statistic 15.0 Software (SPSS Inc., Chicago, Illinois, USA). Comparisons were conducted between control and treated groups with student's t -test, $*p < 0.05$ was considered significant.

RESULTS

Characterization of EBE-UV light sources

The diameter of the front-edge of UV light source is 50 mm, and the length of the whole light source is 155 mm. The emission spectrum is shown in Fig. 3, which indicates a core wavelength of 241 nm with a half-peak width of 15 nm. The photoelectric conversion efficiency was determined to be 4.01%. After 1000-h operation, the photoelectric conversion efficiency will be reduced by about 75%. The irradiance at different distances from the light source is shown in Table 1, which decreases gradually with the increase in distance.

Evaluation of sterilization effect

To evaluate the microorganism-killing effect of deep-UV light, four strains of microorganisms (yeast, Gram-positive and Gram-negative bacteria) were irradiated with 241 nm UV at different doses.

It could be seen that the sterilization efficiency of this EBE-UV light was dose-dependent, and all the microorganisms could be killed under the irradiation lower than $66.6 \text{ mW}\cdot\text{s}/\text{cm}^2$. As shown in Fig. 4a, the most tolerant microorganism was *C. albicans*, while *E. coli* was the most easily killed bacteria (Fig. 4d). The tolerance of *P. aeruginosa* and *S. aureus* was found to be between *C. albicans* and *E. coli* (Fig. 4bc).

Sterilization mechanism

The changes of ROS curve in the four microorganisms after UV treatment were shown in Fig. 5a. As the irradiation time and dose increase, the levels of ROS increase to different degrees for each microorganism. To more intuitively show the effect of irradiation on cells, the fluorescence intensity of DCF in cells was photographed by fluorescence microscopy in the experiment, and the results were shown in the following Fig. 5b, which became brighter with the increase of treatment time. Surprisingly, no production of ozone was detected during the treatment of EBE-UV lights, as the data kept below zero during the detection. In addition, significant DNA damages were noticed after UVC irradiation, as DNA migration exhibited an obvious comet style (Fig. 6 and Table 2).

DISCUSSION

With the development of science and technology, the demands for human health continue to increase. As an important environmental pollutant, mercury is posing a huge threat to human health due to their extensive applications in the industry²⁰. On 19 January 2013, the United Nations Environment Programme adopted Minamata Convention, to reduce the releasing of mercury in the world²¹. For the UV light sources, the convention clearly states that after 2020, low-cost mercury lamps will be unavailable. Hence all countries are developing high-efficiency and mercury-free UV light sources, to occupy a huge market including lighting, sterilization, and wastewater treatment.

In this study, a new sterilization device was constructed with new mercury-free UV sources. The lamp has a maximum emission wavelength of 241 nm with a half-width of 15 nm. The photoelectric conversion efficiency was calculated to be 4%. After improvement on the matrix, much higher photoelectric conversion efficiency of even 12% could be achieved, which is much higher than LG's commercial products (data to be published).

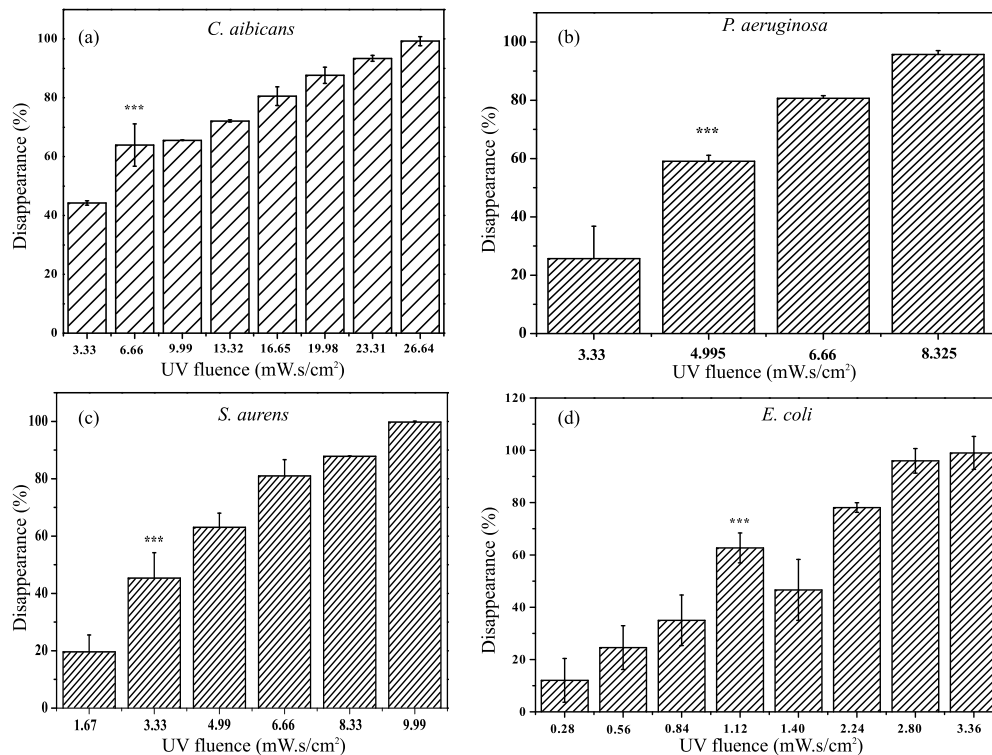


Fig. 4 The sterilization efficiency at 241 nm was examined by disappearance of (a) *C. albicans*, (b) *P. aeruginosa*, (c) *S. aureus*, and (d) *E. coli*. Data are expressed as means \pm SD of 3 samples, *** p < 0.001 compared with untreated control.

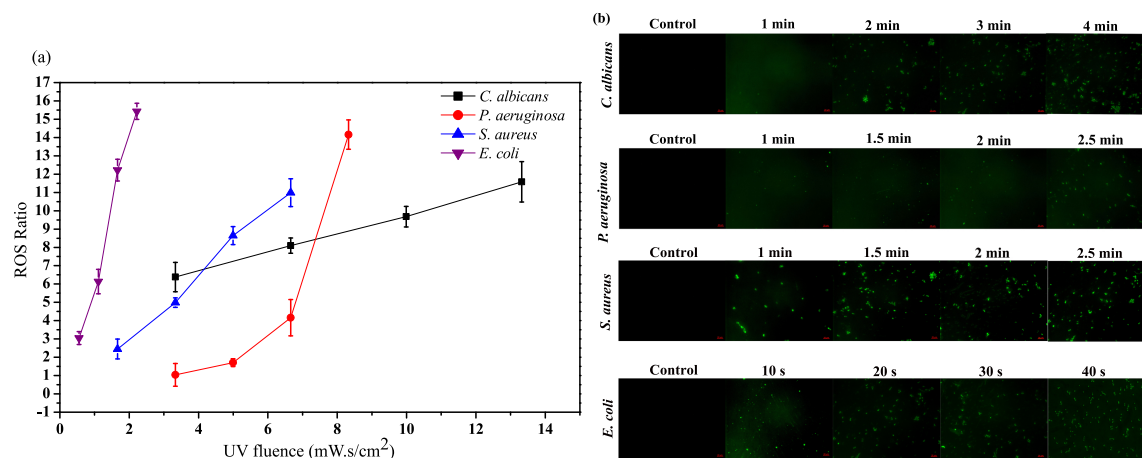


Fig. 5 (a) Intracellular ROS concentration after the treatment with 241 nm EBE-UV lamp in yeast, Gram-positive, and Gram-negative bacteria: ROS value of *C. albicans* (■), *P. aeruginosa* (●), *S. aureus* (▲), and *E. coli* (▼). (b) DCF fluorescence produced by bacteria with fluorescence microscope.

In the previous reports, the effective radiation power of conventional sterilization lamp (254 nm) was 150 mJ/cm² (1.5×10^3 mW·s/cm²), which could kill *C. albicans* up to 10^{-5} CFU/ml²². The dose used by Mohr H and Gravemann U was even higher,

300 mJ/cm² (3.0×10^3 mW·s/cm²) to inactivate 10 bacteria species in platelet concentrates²³. On the other hand, Dotson et al used doses from 0.1–0.2 J/cm² (1.0×10^3 to 2.0×10^3 mW·s/cm²) for drinking water disinfection²⁴. All these irradiation

Table 2 Analytical results of comet assay.

Sample	L-head (μm)	L-tail (μm)	L-comet (μm)	Head-DNA (%)	Tail-DNA (%)	Tail moment	Olivetail moment
<i>C. albicans</i> 0 min	27.0 \pm 2.4	4.3 \pm 0.6	31.4 \pm 3.3	97.53 \pm 3.96	2.46 \pm 0.85	0.09 \pm 0.02	0.32 \pm 0.02
<i>C. albicans</i> 1 min	31.6 \pm 3.8	37.7 \pm 4.0*	69.3 \pm 9.8*	73.33 \pm 5.95	26.66 \pm 3.05*	8.93 \pm 2.08*	9.20 \pm 2.92*
<i>C. albicans</i> 3 min	27.3 \pm 3.6	33.5 \pm 5.5*	60.8 \pm 4.2	73.54 \pm 8.57	26.45 \pm 3.43*	10.72 \pm 1.99*	4.03 \pm 0.12*
<i>P. aeruginosa</i> 0 min	25.7 \pm 3.4	3.0 \pm 1.1	28.7 \pm 3.7	99.95 \pm 8.78	0.04 \pm 0.02	0.02 \pm 0.003	0.01 \pm 0.09
<i>P. aeruginosa</i> 1 min	23.9 \pm 3.6	21.7 \pm 4.8*	45.7 \pm 3.3	79.37 \pm 6.99	20.62 \pm 3.01*	4.33 \pm 2.02*	3.93 \pm 1.33*
<i>P. aeruginosa</i> 2 min	19.7 \pm 3.9	29.8 \pm 6.2*	49.5 \pm 4.8	38.10 \pm 4.22*	61.89 \pm 5.78*	17.95 \pm 2.04*	9.98 \pm 1.96*
<i>S. aureus</i> 0 min	27.1 \pm 2.4	3.7 \pm 1.6	30.7 \pm 7.6	99.93 \pm 12.55	0.06 \pm 0.45	0.009 \pm 0.0003	0.009 \pm 0.0003
<i>S. aureus</i> 0.5 min	26.0 \pm 8.8	18.7 \pm 7.3*	44.7 \pm 6.9	84.28 \pm 7.98	15.71 \pm 4.02*	2.82 \pm 1.78*	2.73 \pm 1.71*
<i>S. aureus</i> 2 min	25.6 \pm 5.8	50.9 \pm 7.4*	76.5 \pm 9.7*	63.83 \pm 4.72	36.16 \pm 3.28*	18.08 \pm 9.14*	12.81 \pm 7.65*
<i>E. coli</i> 0 min	23.2 \pm 3.3	4.0 \pm 1.4	27.2 \pm 4.1	99.97 \pm 9.38	0.02 \pm 0.01	0.007 \pm 0.003	0.003 \pm 0.002
<i>E. coli</i> 10 s	19.4 \pm 4.8	3.9 \pm 2.4	23.4 \pm 8.6	99.92 \pm 27.72	0.07 \pm 0.02	0.002 \pm 0.001	0.007 \pm 0.006
<i>E. coli</i> 40 s	19.4 \pm 4.0	9.6 \pm 2.1*	28.9 \pm 5.1	74.16 \pm 8.23	25.83 \pm 7.77*	2.32 \pm 1.54*	2.56 \pm 1.35*

* $p < 0.05$ versus control.

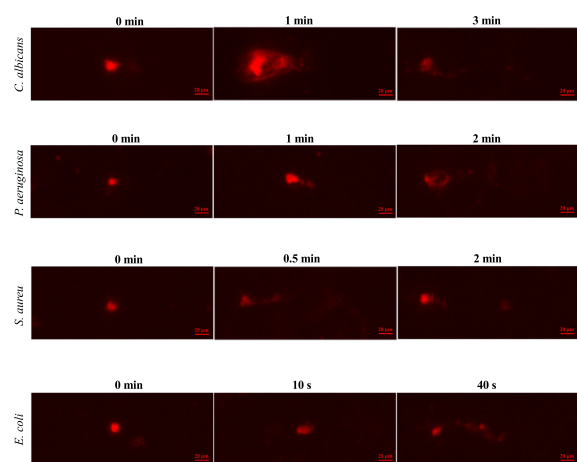


Fig. 6 Representative comet assay images for the four strains: *C. albicans*, *P. aeruginosa*, *S. aureus*, and *E. coli* after the treatment with EBE-UV light.

doses were much higher than that in this experiment, where the new UV sources killed all the four microorganisms after irradiation of 20 min and the dose reached 66.6 $\text{mW} \cdot \text{s}/\text{cm}^2$. Such phenomenon could be due to the narrow spectral peak at 241 nm compared with broad-spectrum of traditional lamps.

According to literature, DNA damage, ROS effects, and production of ozone could be the reasons of UV sterilization. In this experiment, ROS effects and DNA damages have been found in this experiment (Fig. 5 and Fig. 6). However, no ozone was detected after the irradiation of UV lights for 20 min. Such phenomenon could be occurred on the fact that the emission spectrum of EBE lights does not contain 185 nm, which ionizes the air to

generate ozone²⁵. Although ozone can be useful for sterilization, it has strong oxidizing properties, which can cause ageing of equipment and is not suitable for human environment^{26,27}. In this respect, the application of new UV light sources could be advantageous.

CONCLUSION

In this paper, a novel sterilization device was constructed with EBE-UV light sources, which generated UV light with an electron beam to excite $\text{YPO}_4:\text{Bi}^{3+}$ material. This device had a narrow emission peak (241 ± 25 nm), high photoelectric conversion efficiency (4.01%), environmental friendliness (without mercury) and low cost (around 0.5 \$/mW). This device exhibited an excellent sensitization effect at 15 cm from the light source, with oxidative stress as the major mechanism. Hence it has great application prospects for the surface sterilization of objects.

Acknowledgements: This work was supported by grants from National Science and Technology Major Project of China (2017ZX10302301-003) and National Key R&D Programme of China (2017YFF0108600 & 2017YFC0110400).

REFERENCES

1. Rozhansky IV, Zakheim DA (2006) Analysis of dependence of electroluminescence efficiency of AlInGaN LED heterostructures on pumping. *Phys Status Solidi C* **3**, 2160–2164.
2. Gayan E, Serrano MJ, Pagan R, Alvarez I, Condon S (2015) Environmental and biological factors influencing the UV-C resistance of *Listeria monocytogenes*. *Food Microbiol* **46**, 246–253.

3. Chen J, Loeb S, Kim JH (2017) LED revolution: fundamentals and prospects for UV disinfection applications. *Environ Sci Water Res Technol* **3**, 188–202.
4. Yoo ST, Hong JH, Kang JS, Park KC (2018) Deep-ultraviolet light source with a carbon nanotube cold-cathode electron beam. *J Vac Sci Technol B* **36**, ID 02C103.
5. De Volder MF, Tawfik SH, Baughman RH, Hart AJ (2013) Carbon nanotubes: present and future commercial applications. *Science* **339**, 535–539.
6. Hirayama H, Maeda N, Fujikawa S, Toyoda S, Kamata N (2014) Recent progress and future prospects of AlGaIn-based high-efficiency deep-ultraviolet light-emitting diodes. *Jpn J Appl Phys* **53**, ID 100209.
7. Song K, Mohseni M, Taghipour F (2016) Application of ultraviolet light-emitting diodes (UV-LEDs) for water disinfection: a review. *Water Res* **94**, 341–349.
8. Ge CQ, Xie CS, Hu ML, Gui YH, Bai ZK, Zeng DW (2007) Structural characteristics and UV-light enhanced gas sensitivity of La-doped ZnO nanoparticles. *Mater Sci Eng B* **141**, 43–48.
9. Oto T, Banal RG, Kataoka K, Funato M, Kawakami Y (2010) 100 mW deep-ultraviolet emission from aluminium-nitride-based quantum wells pumped by an electron beam. *Nat Photonics* **4**, 767–770.
10. Shatalov M, Sun WH, Lunev A, Hu XH, Dobrinsky A, Bilenko Y, Yang JW, Shur M, et al (2012) AlGaIn deep-ultraviolet light-emitting diodes with external quantum efficiency above 10%. *Appl Phys Express* **5**, ID 082101.
11. Watanabe K, Taniguchi T, Niiyama T, Miya K, Taniguchi M (2009) Far-ultraviolet plane-emission handheld device based on hexagonal boron nitride. *Nat Photonics* **3**, 591–594.
12. Ichikawa N, Ikeda K, Honda Y, Taketomi H, Kawai K, Suzuki T (2016) Development of a UV light source using Pr:LuAG thin film pumped by electron beam. *Electron Commun Jpn* **99**, 33–39.
13. Sousa AM, Machado I, Nicolau A, Pereira MO (2013) Improvements on colony morphology identification towards bacterial profiling. *J Microbiol Methods* **95**, 327–335.
14. Barboza DD, Martins LCA, Correa TQ (2018) Photodynamic inactivation of *Staphylococcus aureus* and *Escherichia coli* using a new bacteriochlorin as photosensitizer. In: Kessel DH, Hasan T (eds) *Optical Methods for Tumor Treatment and Detection - Mechanisms and Techniques in Photodynamic Therapy 27th*, California, USA.
15. Narita K, Asano K, Morimoto Y, Igarashi T, Hamblin MR, Dai TH, Nakane A (2018) Disinfection and healing effects of 222-nm UVC light on methicillin-resistant *Staphylococcus aureus* infection in mouse wounds. *J Photochem Photobiol B* **178**, 10–18.
16. Bagattini M, Buonocore R, Giannouli M, Mattiacci D, Bellopede R, Grimaldi N, Nardone A, Zarrilli R, et al (2015) Effect of treatment with an overheated dry-saturated steam vapour disinfection system on multidrug and extensively drug-resistant nosocomial pathogens and comparison with sodium hypochlorite activity. *BMC Res Notes* **8**, ID 551.
17. Li JH, Wang G, Zhu HQ, Zhang M, Zheng XH, Di ZF, Liu XY, Wang X (2014) Antibacterial activity of large-area monolayer graphene film manipulated by charge transfer. *Sci Rep* **4**, ID 4359.
18. Soares SS, Gutierrez-Merino C, Aureliano M (2007) Mitochondria as a target for decavanadate toxicity in *Sparus aurata* heart. *Aquat Toxicol* **83**, 1–9.
19. Lanier C, Bernard F, Dumez S, Leclercq J, Lemiere S, Vandenbulcke F, Nesslany F, Platel A, et al (2016) Combined effect of Cd and Pb spiked field soils on bioaccumulation, DNA damage, and peroxidase activities in *Trifolium repens*. *Environ Sci Pollut Res* **23**, 1755–1767.
20. Beck SE, Ryu H, Boczek LA, Cashdollar JL, Jeanis KM, Rosenblum JS, Lawal OR, Linden KG (2017) Evaluating UV-C LED disinfection performance and investigating potential dual-wavelength synergy. *Water Res* **109**, 207–216.
21. Gibb H, O'Leary KG (2014) Mercury exposure and health impacts among individuals in the artisanal and small-scale gold mining community: a comprehensive review. *Environ Health Perspect* **122**, 667–672.
22. Buonanno M, Stanislauskas M, Ponnaiya B, Bigelow AW, Randers-Pehrson G, Xu Y, Shuryak I, Smilenov L, et al (2013) 207-nm UV light - a promising tool for safe low-cost reduction of surgical site infections. I: in vitro studies. *PLoS One* **8**, ID e76968.
23. Mohr H, Gravemann U, Bayer A, Mueller TH (2009) Sterilization of platelet concentrates at production scale by irradiation with short-wave ultraviolet light. *Transfusion* **49**, 1956–1963.
24. Dotson AO, Rodriguez CE, Linden KG (2012) UV disinfection implementation status in US water treatment plants. *J Am Water Works Assoc* **104**, 318–324.
25. Szeto W, Li JT, Huang HB, Leung DYC (2018) VUV/TiO₂ photocatalytic oxidation process of methyl orange and simultaneous utilization of the lamp-generated ozone. *Chem Eng Sci* **177**, 380–390.
26. Galante R, Ghisleni D, Paradiso P, Alves VD, Pinto TJA, Colaco R, Serro AP (2017) Sterilization of silicone-based hydrogels for biomedical application using ozone gas: comparison with conventional techniques. *Mater Sci Eng C* **78**, 389–397.
27. Wang YZ, Wang HY, Li XS, Liu DX, Jiang YF, Sun ZH (2013) O₃/UV synergistic aging of polyester polyurethane film modified by composite UV absorber. *J Nanomater* **2013**, ID 169405.